

Electronic Supplementary Information for

**A high efficiency approach for titanium surface
antifouling modification: PEG-o-quinone linked
with titanium via electron transfer process**

*Songtao Liu, Lijuan Chen, Lin Tan, Fuhu Cao, Longchao Bai, Yanmei Wang**

CAS Key Laboratory of Soft Matter Chemistry, Department of Polymer Science and
Engineering, University of Science and Technology of China, 230026, Hefei, People's

Republic of China

1. Materials

Poly (ethylene glycol) methyl ether (mPEG-OH, ca. 2,000, flakes), N-hydroxysuccinimide (NHS, 98.0%), N, N'-dicyclohexylcarbodiimide (DCC), 3, 4-dihydroxy-L-phenylalanine (L-DOPA, $\geq 98\%$, TLC), dopamine hydrochloride were purchased from Sigma-Aldrich (St. Louis, MO, USA). Sodium tetraborate decahydrate ($\text{Na}_2\text{B}_4\text{O}_7 \cdot 10\text{H}_2\text{O}$, $\geq 99.5\%$), sodium hydroxide (NaOH, AR), concentrated hydrochloric acid (HCl, AR), magnesium sulfate anhydrous (MgSO_4 , AR), potassium bisulfate (KHSO_4 , AR), sodium chloride (NaCl, AR), potassium chloride (KCl, AR), disodium hydrogen phosphate (Na_2HPO_4 , AR), monopotassium phosphate (KH_2PO_4 , AR) were purchased from Sinoreagent (Shanghai, China). 1-Hydroxy-benzotriazole (HOBt, 99%), O-(benzotriazolyl)-N, N, N', N'-tetramethyluronium hexafluorophosphate (HBTU, $\geq 98\%$) were purchased from Aladdin (Shanghai, China). Methanesulfonyl chloride was purchased from Guangfu Fine Chemical Research Institute (Tianjin, China). Triethylamine (TEA), dichloromethane (DCM), dioxane, N, N-dimethylformamide (DMF) were purified before use.

2. The preparation and characterization of PEG-catechols^{1,2}

Synthesis of PEG-DOPA(COOH) (P1): A solution of $\text{Na}_2\text{B}_4\text{O}_7$ (20 mL, 0.1 M) and L-DOPA(0.4 g) were subsequently added into a 50 mL reaction flask and stirred at room temperature under nitrogen, and then mPEG-NHS (1 mmol) was dissolved in 2 mL acetone and added into above reaction flask, and then the mixture was stirred at room temperature. After 20 h, 1 M HCl was added into the reaction flask to adjust the pH value

of the mixture until $\text{pH} \approx 2$, and then the mixture was extracted using DCM for three times (50 mL each time) and all of DCM phase was collected. The obtained DCM phase was concentrated by using a rotary evaporator. The concentrated phase was precipitated in cold methanol (three times) and filtered; the filtrate was dried in a vacuum at room temperature, and then mPEG-DOPA(COOH)(P1) was obtained. ^1H NMR (300 MHz, DMSO- D_6 /TMS) (Fig. S1a): δ 12.72 (1H, -COOH), 8.71 (1H, -OH), 8.66 (1H, -OH), 7.59 (1H, -NH-), 6.67-6.40 (3H, $\text{C}_6\text{H}_3(\text{OH})_2$ -), 4.42 (1H, $\text{C}_6\text{H}_3(\text{OH})_2\text{-CH}_2\text{-CH}(\text{COOH})\text{-NH-C(O)-}$), 3.85 (2H, -C(O)CH₂-), 3.60-3.35 (PEO), 3.26 (3H, CH₃O-), 2.74-2.96 (2H, $\text{C}_6\text{H}_3(\text{OH})_2\text{-CH}_2\text{-CH}(\text{COOH})\text{-NH-C(O)-}$).

PEG-DOPA(NH₂) (P2): 1 mmol mPEG-NH₂, 0.54 g BOC-DOPA, 0.27 g HOBt, TEA 0.28 mL and 20 mL mixed solution (DCM : DMF = 1:1) were added into 50 mL reaction flask. 0.76 g HBTU was dissolved in 10 mL DCM and added into the reaction flask, and stirred for 20 h at room temperature under nitrogen. After condensing the solution by using a rotary evaporator, the condensing solution was precipitated with cold methanol three times, dried in a vacuum at room temperature, and then PEG-DOPA (NH₂) (P2) was obtained. ^1H NMR (300 MHz, DMSO- D_6 /TMS) (Fig. S1b): δ 8.90 (1H, -OH), 8.32 (1H, -OH), 8.20-7.1 (3H, -NH₂, -NH-), 6.75-6.45 (3H, $\text{C}_6\text{H}_3(\text{OH})_2$ -), 3.85 (1H, $\text{C}_6\text{H}_3(\text{OH})_2\text{-CH}_2\text{-CH}(\text{NH}_2)\text{-C(O)-NH-}$), 3.60-3.40 (PEO), 3.34 (3H, CH₃O-), 2.74-2.96 (2H, $\text{C}_6\text{H}_3(\text{OH})_2\text{-CH}_2\text{-CH}(\text{COOH})\text{-NH-C(O)-}$).

PEG-DA (P3): A solution of Na₂B₄O₇ (20 mL, 0.1 M) was added into 50 mL reaction flask and stirred at room temperature under nitrogen. After that, 0.4 g dopamine

hydrochloride was added, and then mPEG-NHS (1 mmol) was dissolved in 2 mL acetone and added into the reaction flask, and the mixture was stirred at room temperature for 20 h at room temperature under nitrogen. After that, 1 M HCl was used to adjust the solution until $\text{pH} \approx 2$. The solution was condensed by using the rotary evaporator, and then the condensing solution was precipitated with cold methanol three times, dried in a vacuum at room temperature, and then PEG-DA (P3) was obtained. ^1H NMR (300 MHz, DMSO- D_6/TMS) (Fig. S1c): δ 8.66(1H, -OH), 8.55(1H, -OH), 7.8 (1H, -NH-) 6.62-6.40 (3H, $\text{C}_6\text{H}_3(\text{OH})_2$ -), 3.79 (2H, -C(O)-NH- CH_2 -), 3.70-3.35(PEO), 3.25 (3H, CH_3O -), 3.19 (2H, $\text{C}_6\text{H}_3(\text{OH})_2$ - CH_2 - CH_2 (NH $_2$ -), 2.81-2.98 (2H, $\text{C}_6\text{H}_3(\text{OH})_2$ - CH_2 -).

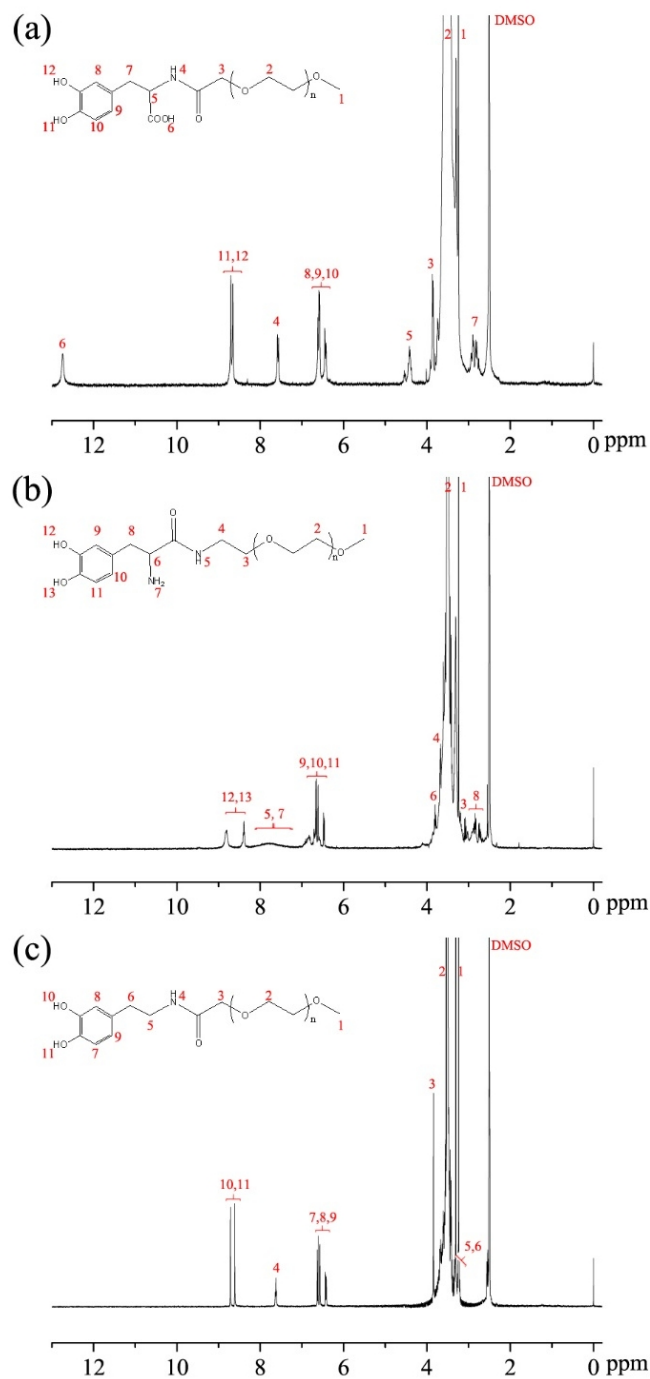


Fig. S1 ¹H-NMR spectra of (a) P1, (b) P2, and (c) P3 in DMSO-D₆.

3. The preparation of an PEG-o-quinone solution

Three types of mPEG-catechols were used to prepare their corresponding o-quinone-

modified PEG. First, 40 mL of a 2 mmol/L P1 MES buffer solution (50 mmol/L MES, pH 6.0, H₂O) and 20 μL of H₂O₂ were added into a two-necked round bottom flask with a condenser, and the solution was then stirred for a specific amount of time at 60 °C. An ultraviolet (UV) and visible spectrophotometer was used to detect the oxidation process by sampling detection every 3 hours until the UV–visible spectrum of the sample did not continue to change. Thus, the PEG-o-DOPAquinone (COOH) (P1') solution was obtained. The procedures for the preparation of PEG-o-DOPAquinone (NH₂) (P2') and PEG-o-quinone (P3') solution from the P2 and P3 solutions, respectively, were the same as the protocol for the P1' preparation. Fig. S2 showed the ultraviolet (UV) and visible spectrophotometer curves of P3'.

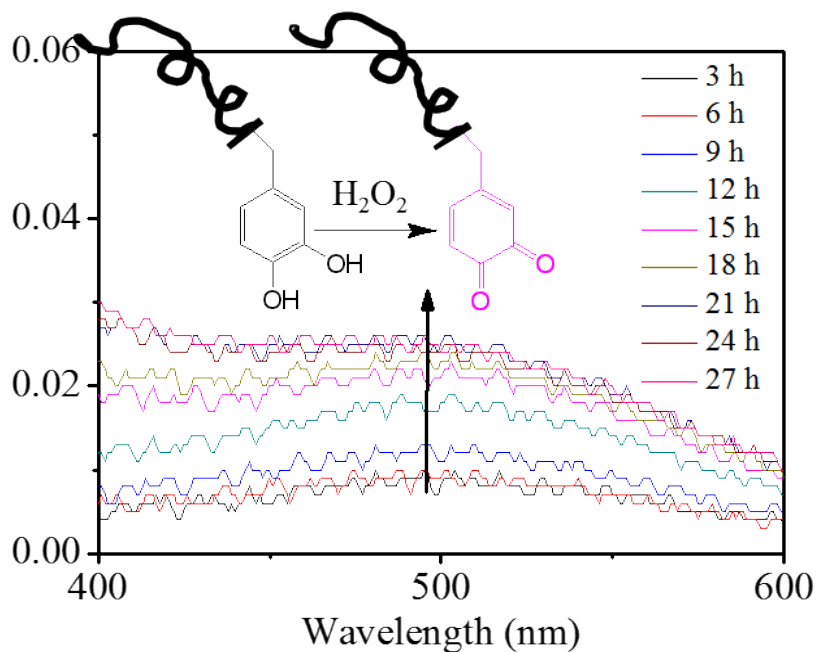


Fig. S2 UV-visible absorption of P3 oxide solution every 3 h. O-quinone has absorption at 400 nm to 600 nm visible light wave range.

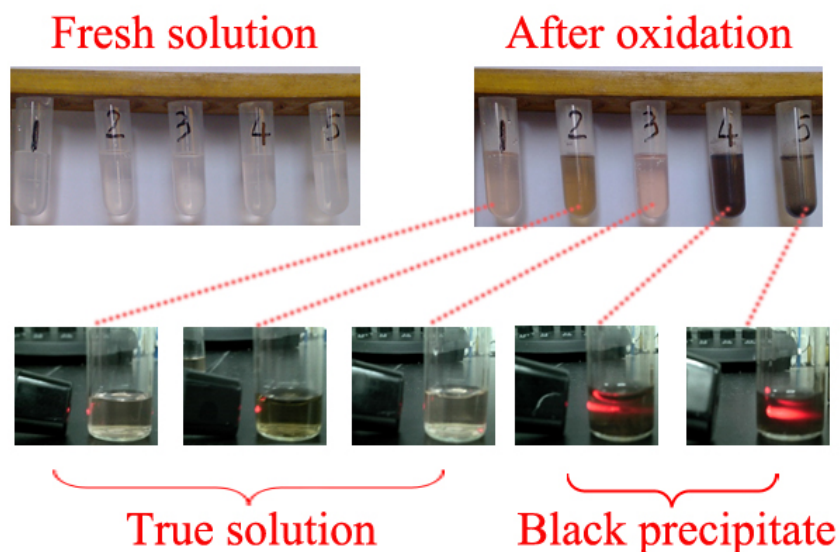


Fig. S3 Comparison of before and after oxidation of P1 (1), P2 (2), P3 (3), dopamine (4), and L-DOPA (5) solution at 60°C.

2 mL ($C = 2$ mM) fresh P1 (1), P2 (2), P3 (3), dopamine (4), and L-DOPA (5) solution (pH 6.0, 50 mM MES buffer) was added into a centrifuge tube, respectively. Each solution was oxidated for 24 hours at 60°C. After that, the color of solution 1 and 3 changed to pink (the color of o-quinone), respectively, and 2 changed to brown (the color of P2"). Black precipitate occurred in the solution 4 and 5, due to the dopamine and DOPA oxidation polymerization. Evidently, the o-quinone segment of the P1', P2', and P3' is chemical stable, due to the steric effect of mPEG chain.

4. Preparation and characterization of titanium substrates

Glass wafers were cut into 1 cm × 2 cm or 1 cm × 1 cm pieces, cleaned in “piranha solution” 1 h (80°C) and water using ultrasonication for 3 × 10 min of treatment, and then dried under a stream of nitrogen in a clean room. The SP-2 sputtering apparatus (product of IMECAS, China) was used for the sputtering of a 200-nm-thick Ti layer under Ar plasma on clean glass wafers to produce the Ti substrates. Next, the Ti substrates (1 cm × 2 cm) were connected with a copper line to obtain the Ti electrode. Cycle voltammetry (CV) scanning was used to produce a stable semi-conductive titanium oxide (TiO₂) nano-film on the Ti substrate surface because the surfaces of fresh Ti substrates require a long time to stabilize under air and an unstable substrate will influence the experiment.

As depicted in Fig. S 4a, the oxidation peak disappeared at the second cycle, this imply that after CV scanning the metal Ti was oxidated to TiO₂. And the XPS spectra of titanium substrate after two cycles CV scanning confirmed that a titanium oxide (TiO₂) nano-film formed on the titanium substrate surface. Moreover, the peak current of CV at about -1.0 V changed little, which verified the electro conductivity changed little though the substrate surface was covered by TiO₂ layer fully.

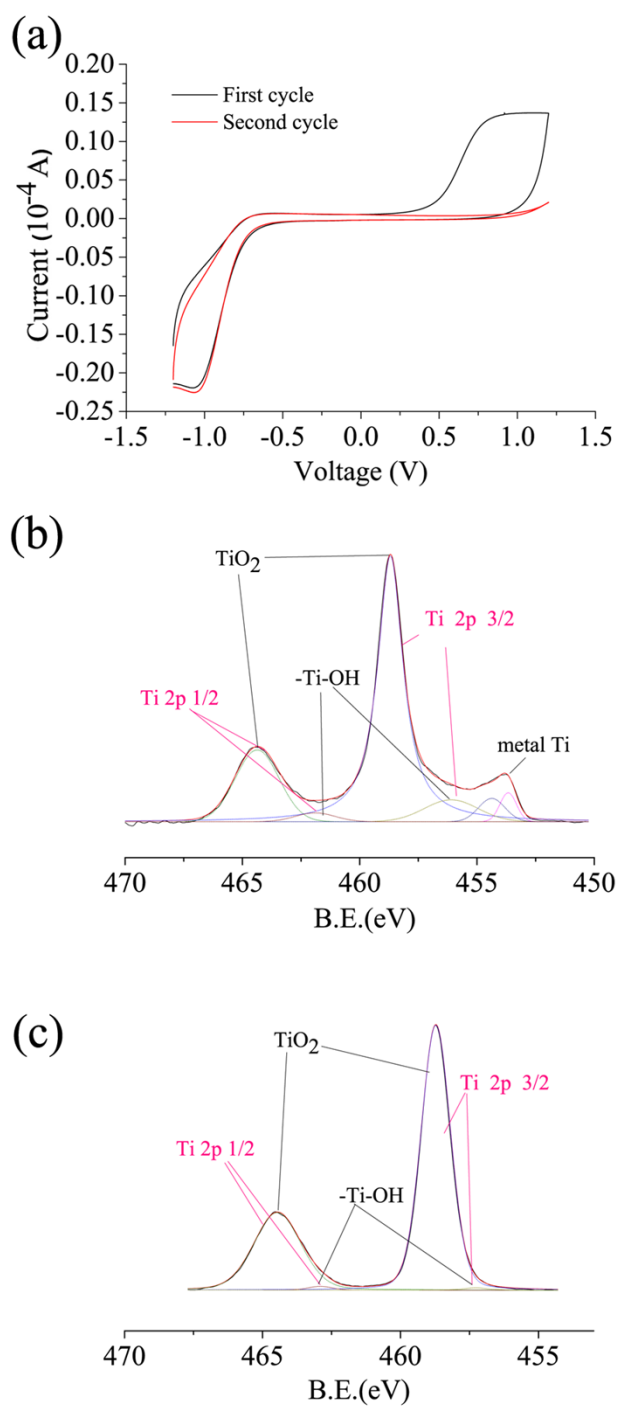


Fig. S4 (a) The electrochemical behavior of fresh titanium substrate in MES buffer. (b) The XPS Ti2p spectra of fresh titanium substrate. (c) The XPS Ti2p spectra of titanium substrate after two cycles CV scanning.

5. Illustration of electrochemical device

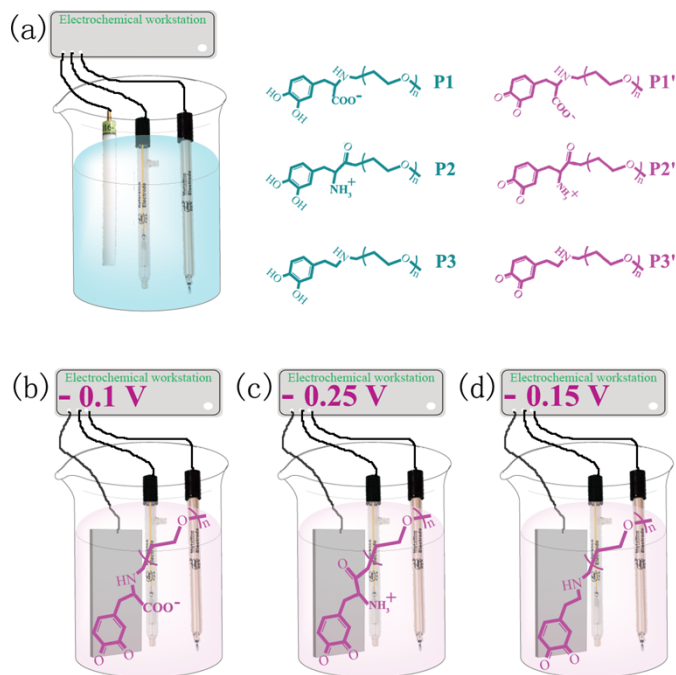


Fig. S5 (a) The device illustration of CV scanning of P1, P2, and P3, and P1', and P2', and P3' solution. (b-d) The devices illustration of CV scanning and potentiostatic electrografting of three kinds of mPEG-o-quinone (P1', P2', and P3').

A CHI600D electrochemical workstation (Chenhua, Shanghai, China) was used to measure the cyclic voltammetry (CV) scans of three types of mPEG-catechol solutions at room temperature. Pt and KCl-saturated Ag/AgCl electrodes were used as the counter and reference electrodes, respectively.³ A glassy carbon electrode was used as the work electrode. Before each scanning, the glass carbon electrode was polished with abrasive paper (grit 2000) and then washed with ethanol and water.⁴ P1, P2, and P3 HEPES2 buffer solutions (0.1 mol/L HEPES, pH 7.4, 150 mmol/L NaCl, H₂O) with different

concentrations were used as the electrolyte. The potential window was -1.2 to 1.2 V (vs. Ag/AgCl), and the scanning rate was 100 mV/s. The illustration of the CV scanning devices is described in Fig. S5.

6. The electrochemical properties of PEG-catechols

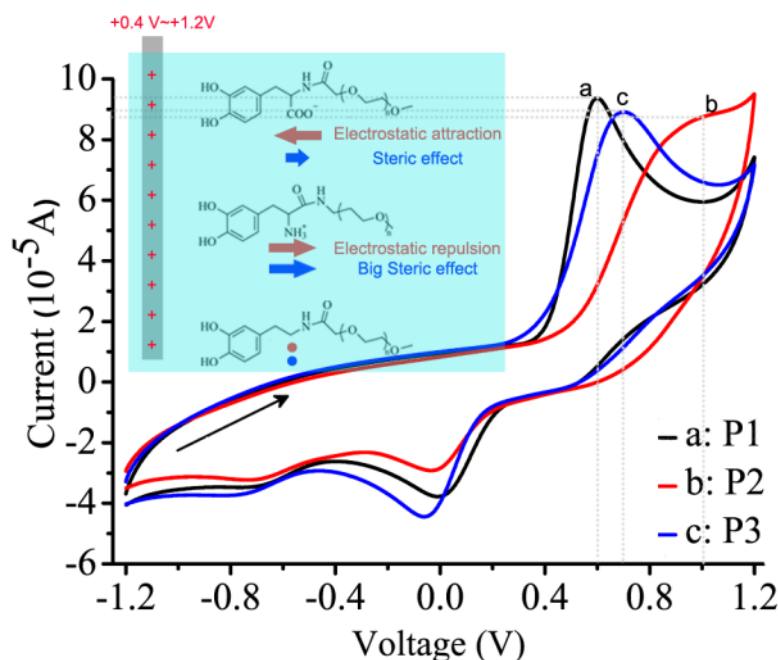


Fig. S6 CVs of P1, P2, P3. All results are measured by three-electrode glass cell with glassy carbon electrode as work electrode. Window: -1.2 to 1.2 V. Scanning speed: 100 mV/s.

As reported,⁵ the efficiency of the grafting of polymer-catechol onto metal oxide surfaces may be strongly influenced by the electrostatic force and the steric effect of different catechol anchor group structures.⁶ In our work, the effects of PEG with different charged head groups on the efficiency of the electrochemical reaction on the electrode surfaces were investigated. The CVs of mPEG-DOPA (COOH) (P1), mPEG-DOPA (NH₂) (P2),

and mPEG-dopamine (P3) HEPES2 buffer solutions with a glassy carbon electrode as the working electrode are displayed in Fig. S6. The different shape of the CV curves in Fig. S6a (P1), Fig. S6b (P2) and Fig. S6c (P3) indicates that the effectiveness of P1, P2, and P3 for the catechol oxidation on electrode is different. As shown in Fig. S6, the oxidation peak current of P1 (with $-\text{COO}^-$) (curve a in Fig. S6) was the highest, followed by P3 (curve c in Fig. S6), and the oxidation peak current of P2 (with $-\text{NH}_3^+$) (curve b in Fig. S6) was the lowest. The oxidation peak potentials of P1, P2, and P3 were 0.6 V, 1.01 V, and 0.7 V, respectively. Usually, both the steric effect of the coating materials and the electrostatic force between the coating materials and the substrates will affect the surface electrochemical reaction rate and the electrografting efficiency. The different head groups of P1, P2, and P3 will produce different steric effects and electrostatic forces.⁷ First, the carboxylate group of P1 and the amino group of P2 impeded the surface reaction of the catechol oxidation due to steric effects; in particular, the positively charged amino group (P2), which easily forms an ionic atmosphere with H_2O molecules in aqueous solution, has a large steric effect. Second, the working electrode surface was positively charged at the oxidation potential (+0.4 V ~ +1.2 V) of the catechol, which resulted in electrostatic attraction with P1 and electrostatic repulsion with P2. As shown in the inset of Fig. S6, the electrostatic attraction enabled P1 to react on the electrode more easily than P3, and the electrostatic repulsion and the large steric effect inhibited the reaction of P2 on the electrode. Evidently, the steric effect and the electrostatic repulsion impeded the surface electrochemical reaction, and the electrostatic attraction between the coating materials

and the substrates could improve the surface electrochemical reaction rate.

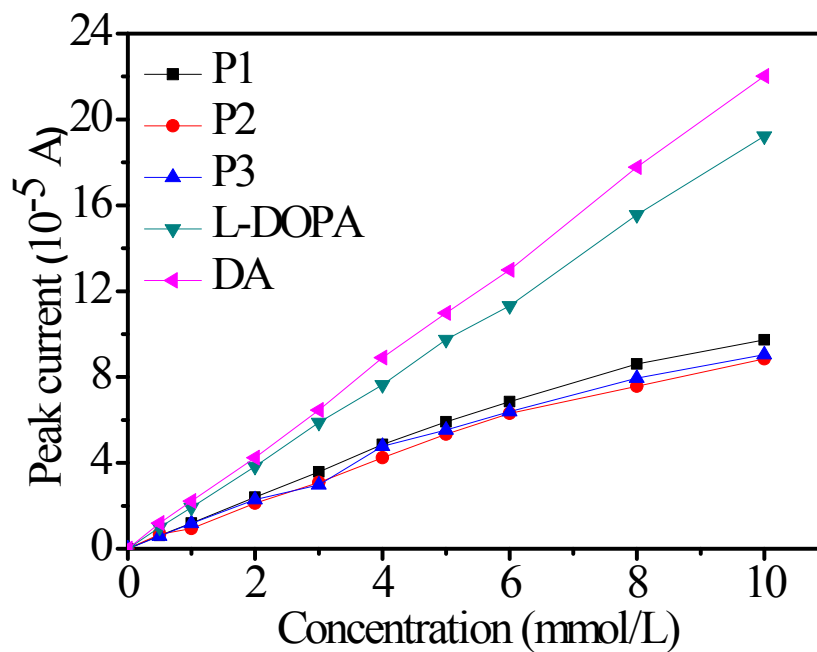


Fig. S7 CV oxidation peak current (background current was deducted) of different concentration of P1, P2, P3, L-DOPA, dopamine. All results are measured by three-electrode glass cell with glassy carbon electrode as work electrode. Window: -1.2 to 1.2 V. Scanning speed: 100 mV/s.

As depicted in Fig. S7, CV oxidation peak current (background current was deducted) of different concentration of P1, P2, P3, L-DOPA, dopamine were verified that the PEG chain have steric effect, because the current of PEG-catechols is lower than that of dopamine and L-DOPA. So the SAMs of PEG-catechol are hard to obtain dense brush on the titanium surfaces.

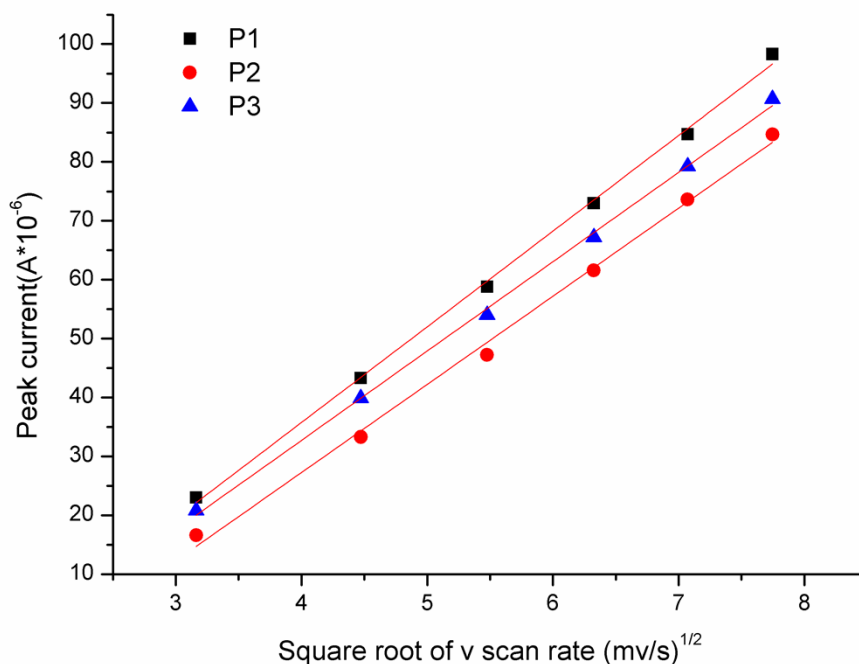


Fig. S8 Peak current vs $v^{1/2}$ (v scan rate) to see the oxidation peak is controlled by diffusion. 10 mmol/L P1, P2, P3 solution were used. All results are measured by three-electrode glass cell with titanium electrode as work electrode. Window: -1.2 to 1.2 V. Scanning speed: 10 mV/s, 20 mV/s, 30 mV/s, 40 mV/s, 50 mV/s, 60 mV/s.

As depicted in Fig. S8, the peak current vs $v^{1/2}$ were linear dependence, which implying the catechol segment of P1, P2, P3 oxidation on the electrode is controlled by diffusion. This is probably due to the steric effect of PEG chain which is difficult to adhere to the electrode surfaces, although the catechol segment has adhesive ability. For PEG-o-quinone, the electrochemical reaction of P1', P2', and P3' on the titanium electrode were also controlled by diffusion, because of the steric effect of PEG chain and low adhesive ability of o-quinone segment.

6.Preparation of e-AMs modified Ti substrates.

The e-AMs of different mPEG-o-quinone were produced using potentiostatic techniques. Potentials of -0.1 V, -0.25 V, -0.15 V were used as the constant potentials of the potentiostatic electrografting of P1', P2', and P3', respectively. Fig. S9 shows the variation of the current with time during the potentiostatic electrografting process over a period of 20 hours. As shown, the current decreased sharply at the very beginning and then decreased slowly after 2 hours. Twenty hours later, the absolute value of the decrease of the current of P3' (curve c) was the highest, followed by that of P1' (curve a). The absolute value of the decrease of the current revealed that the e-AMs of P3' could cover the Ti substrate completely.

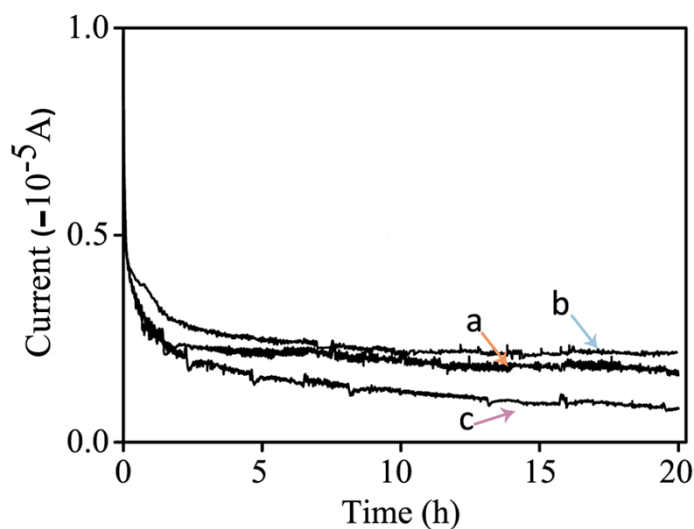


Fig. S9 The current vs. time curves of the potentiostatic electrografting of P1' (a), P2' (b), P3' (c) for 20 hours.

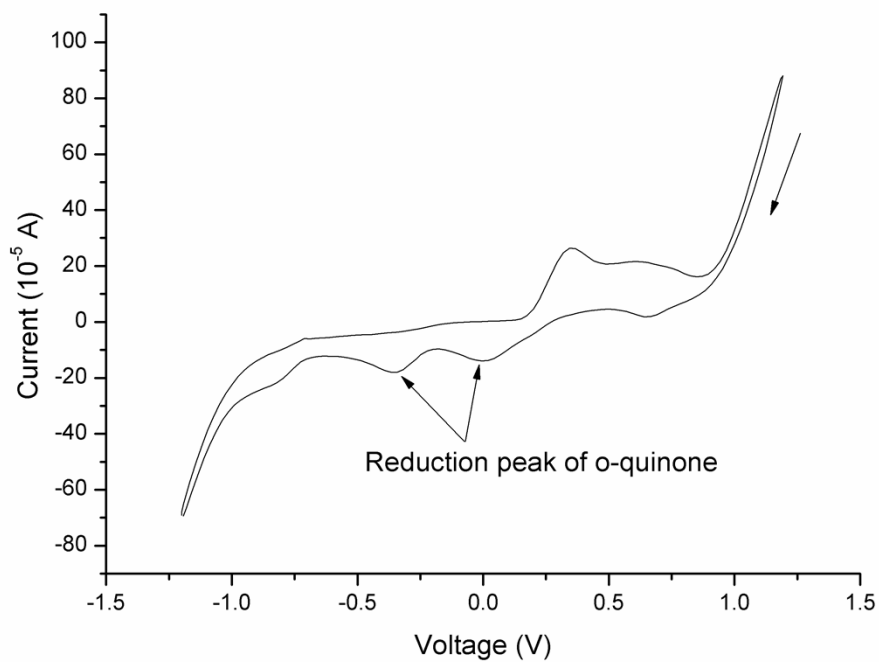


Fig. S10 CV of 2 mmol/L P3' MES buffer solution when Au as work electrode.

As depicted in Fig. S10, the reduction peak current was higher than that of titanium as work electrode (Fig. 1, in the paper), due to the conductivity of Au is better than titanium.

The rate of P3' electroreduction on Au surfaces was higher than on the titanium surfaces.

7.The deconstruction of XPS spectra⁸

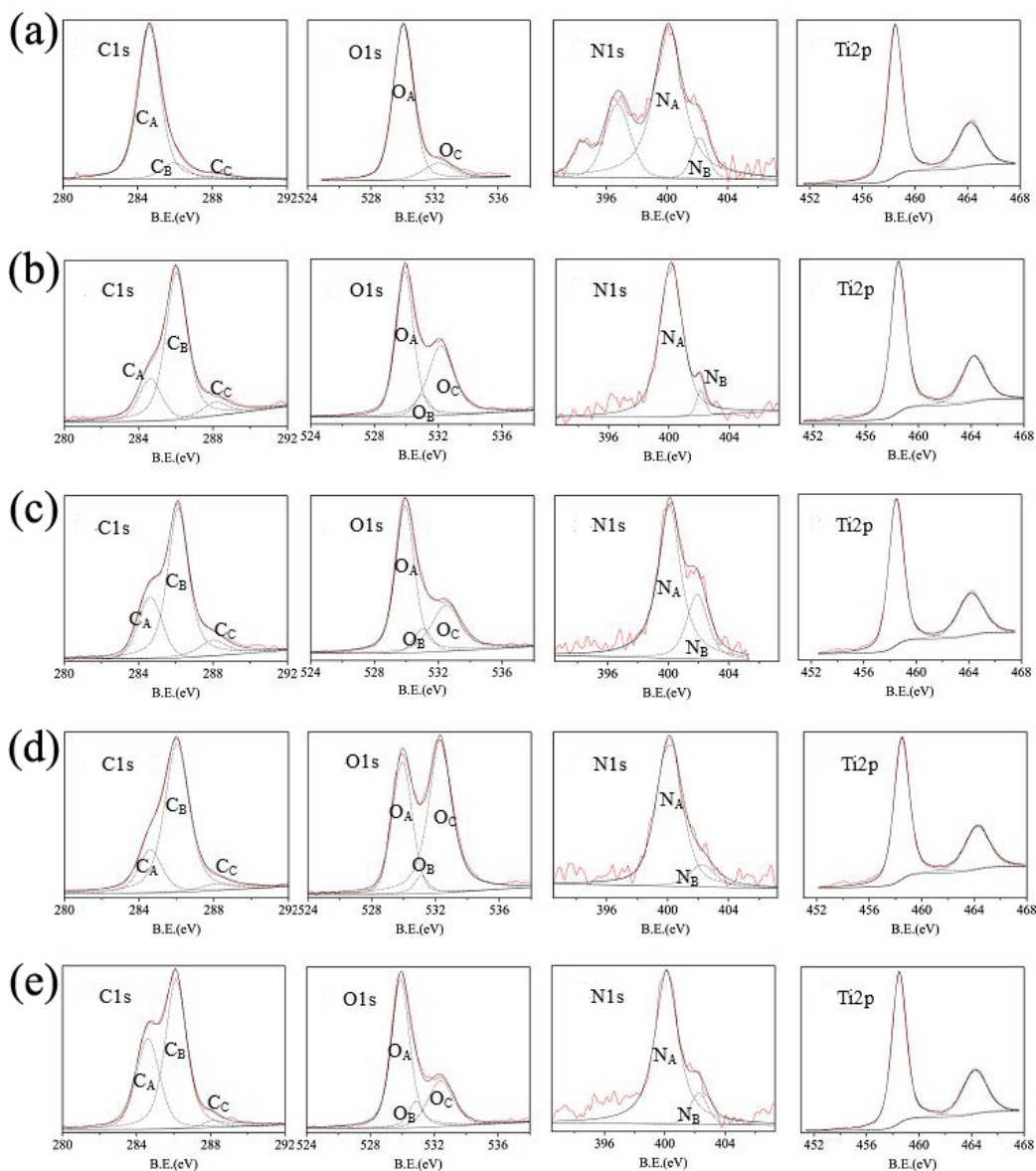


Fig. S11 High resolution C1s, O1s, N1s, and Ti2p XPS spectra of blank substrate (a), e-AMs of P1' modified substrate (b), e-AMs of P2' modified substrate (c), e-AMs of P3' modified substrate (d), SAMs of P3 modified substrate (e). The atomic ratios of different substrate displayed in Table S1.

Table S1 The C, O, N, and Ti atomic concentration for the blank and modified substrates.

	C	O	N	Ti
Blank substrate	15.66	0.87	56.1	27.37
e-AMs of P1'(20h)	46.74	2.89	39.77	10.6
e-AMs of P2'(20h)	41.56	2.57	43.53	12.34
e-AMs of P3'(20h)	59.45	2.67	31.96	5.92
SAMs of P3(20h)	37.42	2.92	44.95	14.71

8. The discussion of AFM image.

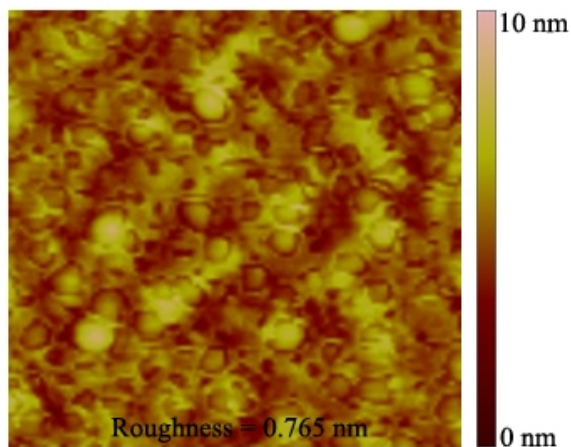


Fig. S12 The AFM height map of 2h electro-assembly modified surface of P3'.

9. The normalized fluorescence intensity values of FITC-BSA adsorption substrate

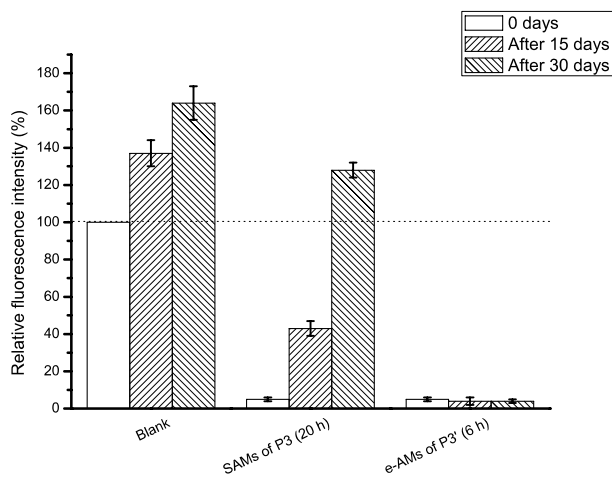


Fig. S13 The normalized fluorescence intensity values of FITC-BSA adsorption substrate, relative to the fluorescence intensity of Fig. 6A (100%).

Table S2 The WCA value change of unmodified and modified Ti substrates incubated in PBS buffer for 0 days, 15 days and 30 days.

Sample	WCA(°)		
	0 day	After 15 days	After 30 days
Untreated Ti	65.7±5.4	\	\
Clean Ti substrate	9.3±4.1	50.9±3	58.0±7.6
Ti (20 h e-AMs, P3')	40.9±1.2	42.8±2.9	41.7±4.2
Ti (6 h e-AMs, P3')	22.2±3.0	24.9±1.5	23.8±1.9
Ti (20 h SAMs, P3)	28.3±0.6	43.9±5.5	54.2±7.8

REFERENCES

- Huang, K.; Lee, B. P.; Ingram, D. R.; Messersmith, P. B., *Biomacromolecules* 2002, **3**, (2), 397-406.
- Lee, B. P.; Dalsin, J. L.; Messersmith, P. B., *Biomacromolecules* 2002, **3**, (5), 1038-1047.
- Belanger, D.; Pinson, J., *Chem. Soc. Rev.* 2011, **40**, (7), 3995-4048.
- Ma, X.; Chao, M.; Wang, Z., *Analytical Methods* 2012, **4**, (6), 1687.
- Zürcher, S.; Wäckerlin, D.; Bethuel, Y.; Malisova, B.; Textor, M.; Tosatti, S.; Gademann, K., *J. Am. Chem. Soc.* 2006, **128**, (4), 1064-1065.
- Malmström, J.; Nieuwoudt, M. K.; Strover, L. T.; Hackett, A.; Laita, O.; Brimble, M. A.; Williams, D. E.; Travas-Sejdic, J., *Macromolecules* 2013, **46**, (12), 4955-4965.
- Ganesh, V.; Pal, S. K.; Kumar, S.; Lakshminarayanan, V., *J. Colloid Inter. Sci.* 2006, **296**, (1), 195-203.
- Dalsin, J. L.; Lin, L.; Tosatti, S.; Vörös, J.; Textor, M.; Messersmith, P. B., *Langmuir* 2004, **21**, (2), 640-646.